Gliadin Nanoparticles as Carriers for the Oral Administration of Lipophilic Drugs. Relationships between Bioadhesion and Pharmacokinetics

Miguel Angel Arangoa,[1] Miguel Angel Campanero,[2] Maria Jesus Renedo,[1] Gilles Ponchel,[3] and Juan Manuel Irache[1,4]

Received April 9, 2001; accepted August 30, 2001

Purpose. The aim of this work was to evaluate the bioadhesive properties of non-hardened gliadin nanoparticles (NPs) and cross-linked gliadin nanoparticles (CL-NP) in the carbazole pharmacokinetic parameters obtained after the oral administration of these carriers.

Methods. A deconvolution model was used to estimate the carbazole absorption when loaded in the different gliadin nanoparticles. In addition, the elimination rates of both adhered and non-adhered nanoparticulate fractions within the stomach were estimated.

Results. Nanoparticles dramatically increased the carbazole oral bioavailability up to 49% and provided sustained release properties related to a decrease of the carbazole plasma elimination rate. The carbazole release rates from nanoparticles (NP and CL-NP), calculated by deconvolution, were found to be of the same order as the elimination rates of the adhered fractions of nanoparticles in the stomach mucosa. In addition, good correlation was found between the carbazole plasmatic levels, during the period of time in which the absorption process prevails, and the amount of adhered carriers to the stomach mucosa.

Conclusion. Gliadin nanoparticles significantly increased the carbazole bioavailability, providing sustained plasma concentrations of this lipophilic molecule. These pharmacokinetic modifications were directly related to the bioadhesive capacity of these carriers with the stomach mucosa.

KEY WORDS: absorption; bioadhesion; bioavailability; deconvolution; gliadin; nanoparticles

INTRODUCTION

A number of drugs remain poorly available when administered by the oral route. Among other reasons, this fact can be related either to 1) a low mucosal permeability for the drug or 2) low solubility for the drug in the mucosal fluids (1–3). In both cases, the drug absorption is poor, and an important fraction of the given dose is eliminated from the alimentary canal before being absorbed.

To circumvent these problems, the association of drugs to polymeric nanoparticulate systems has been proposed. These carriers have the ability for both controlling the release and protecting the loaded drug against its degradation. Moreover, the small particle size (around the micrometer range) allows them to penetrate in the mucus layer and, thus, bind to the underlying epithelium and/or adhere directly to the mucus network (4). These adhesive interactions of the particles with the boundary layer may improve the drug bioavailability by a number of different mechanisms. In this context, nanoparticles may enhance the drug absorption rate by reducing the diffusion barrier between the pharmaceutical dosage form and the site of action or absorption (5). Similarly, they may prolong the residence time of the drug in the gut and, therefore, increase the time when absorption can occur (6,7).

In principle, the evidence of drug absorption is obtained by its appearance in the systemic circulation. For this reason, a pharmacokinetic analysis of the measured plasma drug concentrations is required to characterize the absorptive process. Different experiments in animals have clearly demonstrated that nanoparticles and microparticles can improve the pharmacokinetic properties of several drugs such as vincamine (8), dicumarol (9), insulin (10), and a plasmid DNA named pCMV/β-gal (10). On the other hand, recently performed experiments on human volunteers with riboflavin and furosemide (drugs with a narrow absorption window) loaded in bioadhesive microspheres showed an absorption increase in comparison to non-bioadhesive microspheres. This fact was attributed to a prolongation of the drug residence in the gastrointestinal tract (11,12).

In this work, gliadin nanoparticles were chosen as drug-delivery system because of their strong adhesive capacity with the gastrointestinal mucosa. This high capacity to interact with the mucosa may be explained by gliadin composition. In fact, this protein is rich in neutral and lipophilic residues. Neutral amino acids can promote hydrogen-bonding interactions with the mucosa whereas the lipophilic components can interact with the biologic tissue by hydrophobic interactions (13). In a previous work, we have evaluated the bioadhesive capacity of gliadin nanoparticles when administered by the oral route to animals (14). Gliadin nanoparticles showed a great tropism for the upper gastrointestinal regions. Therefore, 60 min after a single administration of 20 mg of these carriers, approximately 15% of the given dose remained adhered to the stomach mucosa, and their presence in other intestinal regions was very low. In addition, the amount of carriers adhered to the non-glandular region was always significantly higher than to the glandular area of the stomach. To verify the bioavailability increase of lipophilic drugs loaded in bioadhesive nanoparticulate systems as gliadin nanoparticles, carbazole, a lipophilic and fluorescent molecule, was selected as drug model. Therefore, the aim of this work was to correlate the pharmacokinetic parameters of the carbazole administered in gliadin nanoparticles by oral route with the *in vivo* bioadhesive potential of these carriers.

MATERIALS AND METHODS

Materials

Glutaraldehyde grade II (25% aqueous solution), verapamil, trifluoroacetic acid, crude gliadin, and Pluronic F-68®, were purchased from Sigma Chemical Co. (Madrid, Spain). Carbazole and triethylamine were supplied by Aldrich

[1] Centro Galénico, Departamento de Farmacia y Tecnología Farmacéutica, Universidad de Navarra, 31080 Pamplona, Spain.
[2] Servicio de Farmacología Clínica, Clínica Universitaria de Navarra, 31008 Pamplona, Spain.
[3] Physico chimie, Pharmacotechnie, Biopharmacie, UMR CNRS 8612, Université de Paris-Sud, F92296-Châtenay Malabry, France.
[4] To whom correspondence should be addressed. (e-mail: jmirache@unav.es)

0724-8741/01/1100-1521$19.50/0

(Madrid, Spain). All other chemicals used were of reagent grade and obtained from Merck (Darmstadt, Germany).

The experimental volume fraction solubility of carbazole, at 25°C, in water and ethanol was calculated to be 8.05×10^{-7} and 8.99×10^{-3}, respectively (15).

The gliadin used for preparing nanoparticles was isolated and purified from crude gliadin as described previously (16,17). The analysis of the extracted gliadin was performed by reverse-phase high-performance liquid chromtography (HPLC) (16) and high-performance capillary electrophoresis (17). The proportions of the different gliadin fractions were around 10% w/w for ω-gliadin, 52% w/w for α- and β-gliadins, and 37.5% w/w for γ-gliadin.

Carbazole Formulations

For *in vivo* studies, the following pharmaceutical dosage forms containing carbazole were used: 1) propylene glycol solution, 2) aqueous suspension, 3) non-hardened gliadin nanoparticles (NP), and 4) cross-linked gliadin nanoparticles (NP).

To prepare the carbazole solution, the fluorescent marker was dissolved in a propylene glycol:water mixture (75:25 v/v). Aqueous suspensions were prepared by the addition of 0.5 mL of carbazole solution in ethanol (10 mg/mL) to 9.5 mL of water.

Gliadin nanoparticles were prepared by a desolvating procedure described previously (18). In brief, gliadin (100 mg) and carbazole (4.5 mg), were dissolved in 20 mL of an ethanol:water phase (7:3 by vol.) and poured into a stirred saline phase (0.9% NaCl), containing 0.5% Pluronic F-68® as stabilizer. Then, ethanol was eliminated by evaporation under reduced pressure (Büchi R-144, Switzerland) and the resulting nanoparticles purified by centrifugation at 20,000 g for 15 min (Sorvall RC 5C, Newtown, Connecticut). The supernatant was removed and the pellets resuspended in water. This suspension was centrifuged again and, finally, the NP were freeze-dried using a 5% glucose solution as cryoprotector.

On the other hand, some nanoparticle batches were hardened by the addition of 2 mg glutaraldehyde per mg nanoparticle and stirred for 2 h at room temperature before purification and freeze-drying in the same way as described above.

The nanoparticle size and zeta potential were determined by photon correlation spectroscopy in a Zetamaster® (Malvern Instruments, Spain). The zeta potential measurements were performed in a 10^{-4} M HCl solution. On the other hand, the amount of gliadin transformed into nanoparticles was determined by HPLC (16) after sample dissolution in a mixture of acetonitrile and water (7/3 by vol.) containing 0.2% TFA.

Carbazole was quantified by spectrofluorimetry (LS-50 spectrofluorimeter, Perkin Elmer, Boston, Massachusetts) at the excitation wavelength (λ_{ex}): 290 nm and emission wavelength (λ_{ex}): 356 nm.

Administration of Nanoparticulate Formulations and Sample Treatment

Animals used in the experiments were all maintained, treated, and housed according to the guidelines and regulations stipulated by Directive 86/609/EEC. Wistar rats of male sex (mean weight 220 g) were supplied from CIFA (University of Navarra, Pamplona, Spain). Upon arrival, they were housed under normal conditions with free access to food and water. All rats were placed in metabolism cages to prevent coprophagia and fasted overnight but allowed free access to water.

Animals were gavaged with 0.5 mL of the different carbazole formulations containing a dose of 250 μg (1.14 mg carbazole/kg).

All different treatments were divided into two groups of animals. From the first group of animals, blood samples were drawn at 0.08, 0.25, 0.5, 1, 1.5, 2, 2.5, and 3 h post-administration from the ophthalmic venous plexus. Blood samples were centrifuged at 9,000 g for 10 min, and 100 μL of plasma was removed and stored at −40 °C.

The second group of animals was sacrificed by cervical dislocation at 0.25, 0.5, 1, 2, and 3 h post-administration. The abdominal cavity and the stomach were opened immediately, and a blood sample was taken. The stomach was excised with scissors and rinsed with 20 mL of physiological saline to eliminate the lumen contents. Then, the mucosa was cut into segments of 1 cm in length and digested in 1 mL of NaOH 3 M for 24 h. Then, carbazole was extracted with 1.5 mL of methanol, vortexed for 1 min, and centrifuged at 20,000 g for 10 min to eliminate proteins. Furthermore, the rinsing liquids were collected and centrifuged at 20,000 g for 10 min. The resulting residues were dispersed in 0.5 mL of NaOH 3 M and digested overnight (13). Then, the fluorescent marker was extracted as described previously. Extracts also were assayed for carbazole content by spectrofluorimetry.

The developed method was fully validated and, under the experimental conditions described here, no quenching phenomena were found. Recovery (about 94%), linearity, accuracy, sensitivity, selectivity, and reproducibility were the evaluated validation parameters. The calibration curves were linear ($r > 0.997$) over a concentration range of 10–500 ng/mL carbazole. The limit of quantification was calculated to be 10 ng/mL.

Finally, the terminal rate of NP and CL-NP elimination from mucosa and rinsed liquids residues were estimated using the pharmacokinetic software WinNonlin version 1.5 (Scientific Consulting, Inc.).

Plasma Determinations of Carbazole

The amount of carbazole in plasma was determined by HPLC with fluorimetric detection (λ_{ex} 244 nm and λ_{ex} 353) using a Hypersil ODS column (25 × 0.4 cm, 5μ) (Teknokroma, Spain) with methanol and 0.05 M ammonium acetate-acetic acid 4% (w/v)-0.02 M triethylamine (75:25) as mobile phase (flow rate: 1 mL/min) over 6 min. Under these chromatographic conditions, the calibration range for carbazole was drawn between 1 ng/mL and 500 ng/mL. Plasma samples (0.1 mL) were pipetted into a microtube with 40-μL internal standard stock solution (verapamil 0.1 mg/mL) and spiked with 260 μL zinc sulphate 10% (w/v) –0.5 M sodium hydroxide solution. The tube was then vortex mixed for 1 min and centrifuged for 10 min at 15,000 rpm. Finally, the upper layer was separated, was transferred into a chromatographic vial, and 25 μL was injected into the HPLC column.

Pharmacokinetics of Carbazole

A carbazole solution (100 μL) in the mixture propylene glycol:water (75:25) containing 1.14 mg/kg (250 μg), was ad-

ministered by intravenous bolus in the tail vein. The treatment of blood samples was performed in the same way as described before.

Several pharmacokinetic compartment models were evaluated to identify the carbazole pharmacokinetic profile. The possible optional models were 1) the one-compartment model with first-order input and 2) the classic two-compartment model. The Akaique criterion (19) was used to identify the best model.

Pharmacokinetic Analysis of Oral Formulations

To study the disposition of carbazole after the oral administration of different formulations, a model-independent pharmacokinetic analysis was performed using the methods described by Rowland and Tozer (20). Area under the curve (AUC) for serum concentration vs. time plots was calculated by linear trapezoidal rate. The terminal rate of elimination was estimated using the pharmacokinetic software WinNonlin version 1.5 (Scientific Consulting, Inc.). The AUC from the last time point to infinity was estimated by dividing the last measured concentration by the terminal rate of elimination. The maximum plasma concentration, C_{max}, and the time, t_{max}, required to reach C_{max} were obtained from the plasma concentration curve. Finally, the mean residence time was calculated by model-independent statistical moment analysis (20).

Establishment of Relationships between Bioadhesion and Pharmacokinetics

To correlate the bioadhesive potential of gliadin nanoparticles with the pharmacokinetic parameters when administered by the oral route, we proposed a first-order absorption model with the following two components: 1) an instantaneous release component with first order absorption corresponding to free carbazole (k_b) from digested nanoparticles either in luminal fluids or adhered in the mucus and 2) a slow-release component with first-order release and absorption (k_c) corresponding to adhered nanoparticles (Fig. 1).

For foreseeing the carbazole absorption or input function and confirming that hypothesis, a deconvolution model was employed. In linear systems, the deconvolution operations calculate input functions, $I(t)$, using both response $R(t)$ and weighting functions $W(t)$. In the practice, the deconvolution operation can be solved algebraically using Laplace transforms of the follow function (21):

$$I(t) = \frac{R(t)}{W(t)} \quad (1)$$

where $W(t)$ is the exponential equation that defines the plasma carbazole profiles from an instantaneous release formulation (a solution of 250 μg carbazole in 0.5-mL propylene glycol/water 75:25 v/v) administered by oral route and $R(t)$ is the exponential equation that describes plasma carbazole profiles from a slow release formulation administered by the same route (in our case, NP and CL-NP formulations). These exponential equations were obtained by a compartimental analysis of experimental data.

According to the results of the algebraic deconvolution (21), the cumulative input function contains information about the carbazole absorbed amount and rate when released from the nanoparticulate formulations. Moreover, from this input function, it is possible to determine the first-order release constant. The input function was determined using the software DCN-Program (Department of Pharmacy and Pharmaceutical Technology, University of Salamanca, Spain, version 1.0).

Taking into account that the model defined in Figure 1 can be considered as linear, we can write algebraically the deconvolution between the response and weighting functions. Based in this model, two different input functions can be algebraically defined. The first one is related to a single slow release of the active molecule from the pharmaceutical dosage form (see Eq. 2). The second one represents the drug absorption after a biphasic release pattern, characterized by

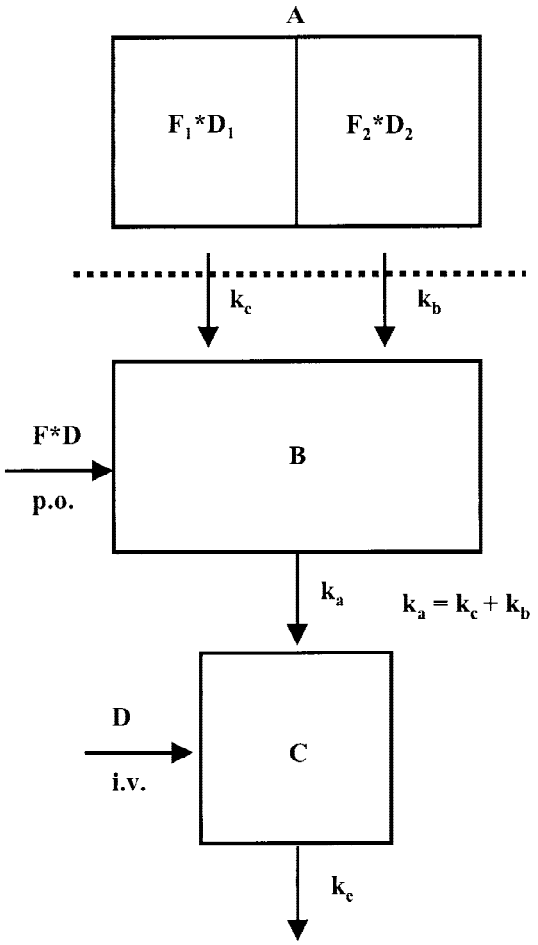

k_a= absorption rate of carbazole
k_b= absorption rate of free carbazole
k_c= absorption rate of carbazole from adhered nanoparticles
k_e= plasma elimination rate of carbazole
D= dose
F= bioavailability

Fig. 1. Hypothesis of the carbazole-loaded gliadin nanoparticles disposition after its oral administration. The intravenous dose (D) is incorporated into compartment C. The dose of the oral solution (F*D) is incorporated into compartment B (absorption compartment). The slow release formulation with a sustained release component (F_1*D_1) and an instantaneous release component (F_2*D_2) are represented by compartment A.

both an instantaneous and a slow release of the loaded molecule in the nanoparticulate carriers (see Eq. 3). These two equations can be wrote as follows:

$$I = FDk_c(1 - e^{-k_c t}) \quad (2)$$

$$I = F_1 D_1 k_c(1 - e^{-k_c t}) + F_2 D_2 \quad (3)$$

where F_1 and D_1 are the bioavailability and dose corresponding to a slow release component, F_2 and D_2 are the fraction of bioavailability and dose corresponding to an instantaneous release component.

Pharmacokinetics-Bioadhesion Correlations

The verification of the hypothesis was performed by two different ways. The former was performed by comparing the pharmacokinetic parameters obtained with the proposed hypothesis and the kinetic parameters obtained from the adhesive interactions of nanoparticles with the stomach mucosa. The second verification procedure was performed by the statistical comparison of the plasma levels, during the period where the absorption process prevails, with the corresponding adhered and non-adhered nanoparticulate fractions in the stomach mucosa.

Statistical Analysis

Parameters were analyzed to determine statistical significance. The mean concentration at each time point was compared for statistical difference using a two-tailed Student's *t* test.

RESULTS

Physicochemical Characterization

Table I summarizes the main physicochemical characteristics of carbazole formulations based on the use of NP and CL-NP.

Pharmacokinetic Profile of Carbazole Formulations

First, the carbazole pharmacokinetic profile had to be elucidated before studying its absorption when released from nanoparticles. For this purpose, propylene glycol:water solutions of the fluorescent marker were administered intravenously. By this route, carbazole displayed a rapid disappearance from the plasma ($k_e = 2.1\ h^{-1}$) and the monocompartimental model appeared to provide the lowest Akaique value. Consequently, this model was chosen for determining the pharmacokinetic parameters associated with intravenous administration.

On the other hand, the plasma concentrations obtained from the oral administration of carbazole aqueous suspensions were low, near the limit of detection of the analytical method (see Fig. 2). Under these conditions, it was not possible to determine the pharmacokinetic parameters (k_e, t_{max}, and C_{max}) and it was considered that the carbazole AUC was around zero because its absorption was negligible.

The plasma profiles and pharmacokinetic parameters of carbazole after the oral administration of NP and CL-NP, respectively are shown in Figure 2 and Table II, respectively. It was interesting to note that the carbazole bioavailability, when administered in nanoparticles, was calculated to be about 40% of the given dose. Similarly, when nanoparticles were cross-linked with glutaraldehyde, the bioavailability of the loaded carbazole increased until 49% of the given dose. Furthermore, the k_e of carbazole in CL-NP was slower than when formulated in non-hardened nanoparticles. Moreover, the carbazole mean residence time, provided by CL-NP, significantly increased in comparison with NP.

Finally, the pharmacokinetic parameters for the carbazole oral solutions in a mixture of propylene glycol and water (75:25 v/v) are displayed in Table II. These experiments were performed to obtain the plasma profile of an instantaneous release formulation, which was necessary for the development of the deconvolution model (see Material and Methods).

Figure 3 shows the accumulative amounts, obtained by deconvolution by means of oral solution subtraction, for both NP and CL-NP. The plot represents a monoexponential function corresponding to Equation 1 (Material and Methods). It appears to be clear that the immediately release com-

Table I. Physicochemical Characteristics of NP[a] and CL-NP

	Size (nm)	Zeta[b] potential (mV)	Yield (%)	Loaded carbazole (μg/mg)
NP	460 ± 19	27.5 ± 0.8	89.6 ± 4.5	12.57 ± 1.23
CL-NP	453 ± 24	24.5 ± 0.5	86.8 ± 5.7	12.23 ± 0.78

[a] NP, non-hardened gliadin nanoparticles; CL-NP, cross-linked gliadin nanoparticles.
[b] Experiment performed in a 10^{-4} M HCl solution.
Values represent the mean ± standard deviation ($n = 6$).

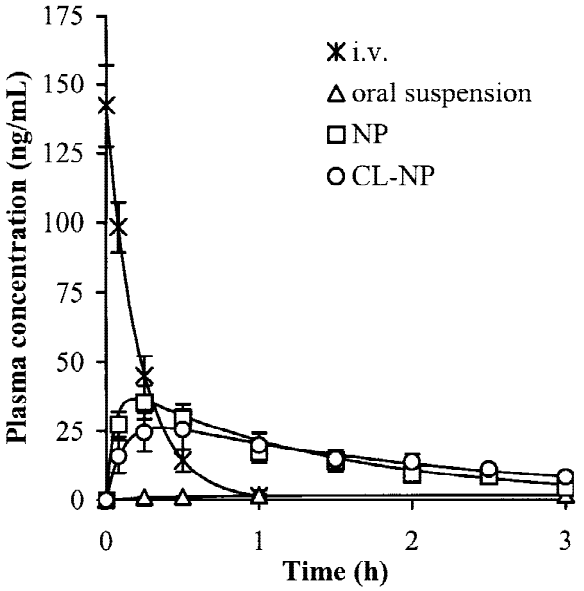

Fig. 2. Mean plasma concentration-time profiles of carbazole after the intravenous single administration of 250 μg as solution (*), oral single administration of 250 μg as aqueous suspension (△), non-hardened gliadin nanoparticles (□), or cross-linked gliadin nanoparticles (○) (n = 12). The lines represent the calculated profiles obtained by nonlinear regression of the data.

Table II. Pharmacokinetic Parameters of Carbazole after Single Administration of 250 μg Carbazole (1.14 mg/kg) by Intravenous Solution of 0.1 mL or Oral Routes (Oral Suspensions, NP[a], CL-NP, and Oral Solution)

	k_e (h^{-1})	t_{max} (h)	C_{max} (ng/mL)	$AUC_{0-\infty}$ (μg h)/L	Mean residence $time_{0-\infty}$ (h)	F (%)	k_c (h^{-1})
Intravenous solution[b]	2.10 ± 0.34	—	—	135.17 ± 17.89	0.81 ± 0.09	—	—
Aqueous suspension[c]	ND	ND	ND	ND	ND	ND	—
NP[d]	0.69* ± 0.12	0.18* ± 0.05	36.64* ± 2.48	54.11 ± 8.53	1.55 ± 0.18	40.03 ± 5.96	0.787
CL-NP[d]	0.46** ± 0.09	0.35** ± 0.09	26.17** ± 2.20	66.26 ± 10.95	2.11 ± 0.16	49.02 ± 7.73	0.588
PG:water solution[e]	0.92 ± 0.16	0.11 ± 0.03	47.24 ± 3.19	54.04 ± 9.11	1.18 ± 0.14	39.98 ± 6.45	—

* $P < 0.05$; ** $P < 0.01$.
[a] NP, non-hardened gliadin nanoparticles; CL-NP, cross-linked gliadin nanoparticles; ND, not determined.
[b] Carbazole (250 μg) in 0.1 mL of propylene glycol:water mixture.
[c] Carbazole (250 μg) dispersed in 0.5 mL of water.
[d] Carbazol (250 μg) loaded in gliadin nanoparticles and dispersed in 0.5 mL of water.
[e] Carbazole (250 μg) in 0.5 mL of propylene glycol:water mixture.

ponent of carbazole from nanoparticles may be considered to be negligible because the intersection with the "y-axis" of the curve was close to zero. From these results, the first-order absorption constant value (k_c) was obtained by extrapolation (Table II). In addition, the absorption rate constant for NP was calculated to be 1.4 times higher than for CL-NP. Consequently, a slower terminal decline in carbazole plasma concentrations was observed with the cross-linked nanoparticles (Fig. 2). This fact agreed with the pharmacokinetic parameters observed for NP and CL-NP, respectively and confirmed the influence of the cross-linkage on the release from gliadin nanoparticles.

Elimination Rate of Adhered and Non-Adhered Nanoparticles

The amount of adhered and non-adhered nanoparticles was estimated from the measurement of the carbazole found in the stomach mucosa (adhered fraction) and in the residues obtained after centrifugation of the rinsing liquids (non-adhered fraction). Figure 4 shows the evolution of the adhered and non-adhered nanoparticulate fractions in the stomach after the oral administration of 20 mg of nanoparticles. From these results, it appeared that NP displayed a higher capacity to strongly interact with the stomach mucosa than CL-NP, although cross-linking nanoparticles remained adhered for a longer time than conventional nanoparticles.

Table III displays the elimination rate of both the adhered (k_{ad}) and the non-adhered (k_{nad}) fractions for NP and CL-NP. For NP, the value of k_{ad} was higher than that obtained for CL-NP. This difference can be due to the cross-linkage with glutaraldehyde. However, the value of $k_{nad}$was greater for CL-NP. This fact may be explained as a consequence of an adsorption-desorption equilibrium where CL-NP would present the lowest adhesive capacity.

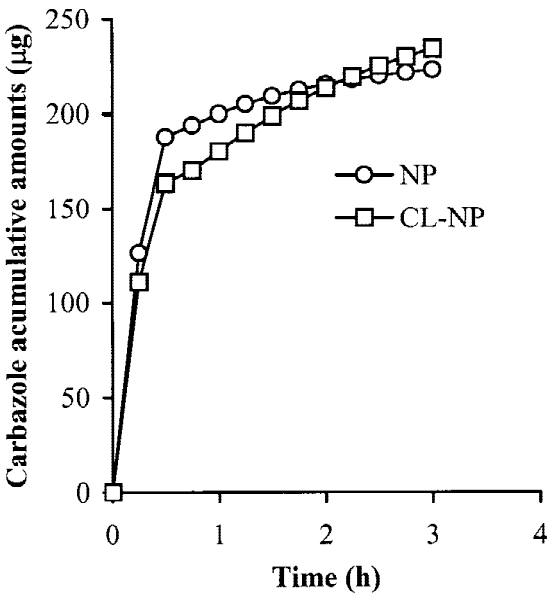

Fig. 3. Accumulative amounts of carbazole obtained from deconvolution for gliadin nanoparticles (○) and cross-linked non-hardened gliadin nanoparticles (□).

Pharmacokinetics-Bioadhesion Correlations

The elimination rates for the adhered (k_{ad}) and the non-adhered (k_{nad}) nanoparticulate fractions in the stomach were

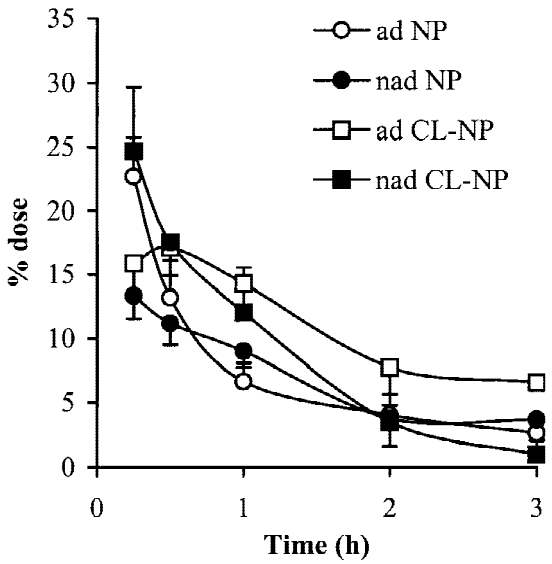

Fig. 4. Recovery of conventional and cross-linked gliadin nanoparticles within the stomach after single oral administration of 20 mg of particles (1.14 mg carbazole/kg). Open symbols represent the adhered fractions (ad) with the stomach mucosa. Close symbols represent the non-adhered fractions (nad). All of these dose fractions are expressed as the percentage of given dose and represent the mean ± standard deviation. (n = 6).

Table III. Terminal Elimination Rates of Adhered (k_{ad}) and Non-adhered Nanoparticulate Fractions (k_{nad}) in the Stomach

	Nanoparticles in stomach		Carbazole plasma levels
	k_{ad} (h^{-1})	k_{nad} (h^{-1})	k_c (h^{-1})
NP[a]	0.782 ± 0.114	0.555	0.787
CL-NP	0.582 ± 0.101	1.151	0.588

Estimations were developed with the pharmacokinetic software WinNonlin version 1.5 (Scientific Consulting, Inc.). The first order absorption constant value (k_c) was obtained from the deconvolution procedure.

[a] NP, non-hardened gliadin nanoparticles; CL-NP, cross-linked gliadin nanoparticles.

compared with the absorption rates (k_c) obtained by deconvolution (see Table III). It was interesting to note that the elimination rates of adhered fractions were of the same order of the absorption rates obtained from the deconvolution procedure.

Finally, the correlation between the amount of adhered carriers to the stomach mucosa during the period of time where the absorption process prevails (mucosa samples of 0.25 and 0.5 h) and their corresponding carbazole plasma levels is shown in Figure 5. Both non-hardened and cross-linked nanoparticles showed good correlation coefficients (0.984 for NP and 0.994 for CL-NP). On the contrary, no correlation was found between non-adhered fractions and carbazole plasma levels (data not shown).

DISCUSSION

Carbazole is a highly lipophilic molecule, with a remarkably low solubility in aqueous milieu, and its oral administration aqueous suspension provided negligible plasma concentrations (Fig. 2). For this reason, this molecule can be considered a good marker to evaluate the bioadhesive properties of drug delivery systems. The oral administration of carbazole loaded in NP or CL-NP significantly increased its absorption. Therefore, the pharmacokinetic parameters and the plasma profiles (see Table II and Fig. 2) clearly showed increases in the AUC related to a significant improve in the carbazole bioavailability when loaded in gliadin nanoparticles.

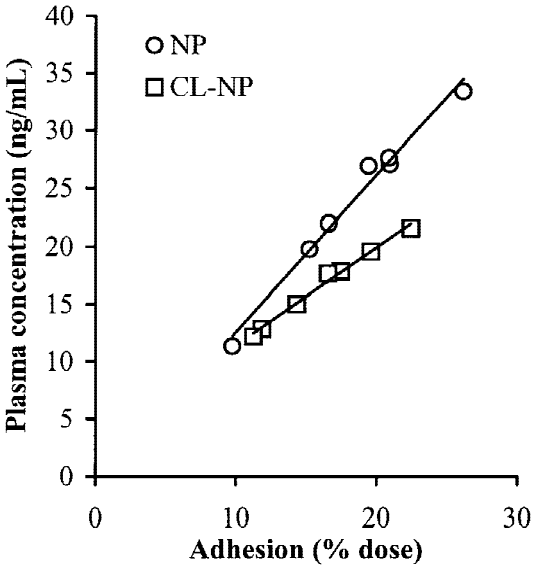

Fig. 5. Statistical comparison between adhered non-hardened gliadin nanoparticles (○) and cross-linked gliadin nanoparticles (□) in the mucosa and their corresponding carbazole plasma concentrations.

Usually, an oral sustained release formulation displays a slower elimination rate (k_e) than the observed for a traditional or immediately release formulation. This fact is a consequence of a slow absorption in comparison with the traditional dosage form (22). In our case, the analysis of the carbazole pharmacokinetic profile after oral administration of nanoparticles shows typically concentration-time data of sustained-release formulations because carbazole k_e from nanoparticles is slower than the carbazole k_e obtained from intravenous administration. Furthermore, the cross-linking process enabled us to increase the carbazole $t_{max}$and to decrease both the marker C_{max} and its k_e. These facts can be related to both 1) a modification in the carbazole absorption rate and 2) an improvement in the sustained release characteristics of carbazole (lower C_{max} and higher t_{max}than for NP) from cross-linked nanoparticles.

The measurement of the absorption extent or bioavailability from a pharmaceutical nanoparticulate system provides useful, but incomplete, information of the absorption process. The drug absorption, from a sustained release formulation administered by the oral route, can be defined in terms of input measured as a combined process of release and systemic absorption. Consequently, additional information on the rate of absorption is needed to obtain a better understanding of the drug input (23). After administration of a sustained release formulation, one of the best approaches to study the drug absorption may be the use of a pharmacokinetic independent-model as the deconvolution model. This model has been successfully applied to the bioavailability studies and for the analysis of release and absorption processes of linear systems (24–26).

The information obtained with a deconvolution model represents the *in vivo* drug release rate from a sustained release formulation (i.e., nanoparticles), rather than a true absorption rate of the drug orally administered. Usually, these drug release rates are very slow first-order processes in comparison with absorption rate values (23). Under these conditions, the release process is the limiting step in the absorption phenomenon, and the deconvolution rate constants are synonymous of the drug released rate from the nanoparticulate system.

The hypothesis proposed in this work has been confirmed by the comparison of the carbazole elimination rates for the adhered and the non-adhered nanoparticulate fractions in the stomach with the deconvolution rate constants (see Table II). This hypothesis implies to assume that once carbazole released from the nanoparticles adhered to the stomach mucosa, it should be immediately absorbed due to its lipophilic character. Taking in an absolute value, the deconvolution rate constants were similar to the corresponding elimination rates of the NP and CL-NP adhered fractions with the stomach mucosa. Moreover, we can conclude that the carbazole absorption is controlled by the bioadhesive interactions of gliadin nanoparticles with the stomach mucosa. Furthermore, this phenomenon is directly related with the bioavailability increase of carbazole for the formulations based on the use of gliadin nanoparticles. On the other hand,

the non-adhered nanoparticulate fractions had not a direct influence in the carbazole absorption rate, although these carriers might act as reservoirs.

Moreover, the adhered and the non-adhered nanoparticulate fractions were statistically compared with the corresponding carbazole plasma concentrations during the period of time in which the absorption process prevailed (see Fig. 5). For both NP and CL-NP formulations, good correlation coefficients were found. These results enabled us to corroborate the proposed hypothesis and to give another clear evidence that the bioadhesive interactions of gliadin nanoparticles with the stomach mucosa are directly responsible for the carbazole absorption.

In summary, gliadin nanoparticles appear to be good pharmaceutical dosage forms for the oral delivery of lipophilic molecules. Therefore, these carriers significantly increased the carbazole bioavailability and provided sustained plasma concentrations of the lipophilic model molecule. All of these results clearly proved that it exists a narrow relationship between the observed pharmacokinetic parameters of carbazole in plasma and the capacity of gliadin nanoparticles in developing bioadhesive interaction with the gut mucosa. Finally, the proposed hypothesis in this work could be applied to elucidate the disposition mechanisms of other bioadhesive formulations.

ACKNOWLEDGMENTS

The first author wishes to thank the "Ministerio de Educacion y Cultura" (Spain) for the grant that enables him to conduct this research.

REFERENCES

1. M. A. Longer, H. S. Ch'ng, and J. R. Robinson. Bioadhesive polymers as platforms for oral controlled drug delivery III: Oral delivery of chlorothiazide using a bioadhesive polymer. *J. Pharm. Sci.* **74**:406–411 (1985).
2. J. Kreuter. Peroral administration of nanoparticles. *Adv. Drug Deliv. Rev*. **7**:71–86 (1991).
3. S. Sakuma, R. Sudo, N. Suzuki, H. Kikuchi, M. Akashi, and M. Hayashi. Mucoadhesion of polystyrene nanoparticles having surface hydrophilic polymeric chains in the gastrointestinal tract. *Int. J. Pharm.* **177**:161–172 (1999).
4. C. Durrer, J. M. Irache, F. Puisieux, D. Duchêne, and G. Ponchel. Mucoadhesion of latexes. II. Adsorption isotherms and desorption studies. *Pharm. Res.* **11**:680–683 (1994).
5. P. K. Gupta, S. H. Leung, and J. R. Robinson. Bioadhesives/ Mucoadhesives in drug delivery to the gastrointestinal tract. In V. Lenaerts, and R. Gurny (eds.), *Bioadhesive Drug Delivery Systems*, CRC Press, Boca Raton. FL; 1990, pp. 65–92.
6. C. M. Lehr. Bioadhesion technologies for the delivery of peptide and protein drugs to the gastrointestinal tract. *Crit. Rev. Ther. Drug Carrier Syst.* **11**:119–160 (1994).
7. S. Sakuma, N. Suzuki, H. Kikuchi, K. I. Hiwatari, K. Arikawa, A. Kishida, and M. Akashi. Oral peptide delivery using nanoparticles composed of novel graft copolymers having hydrophobic backbone and hydrophilic branches. *Int. J. Pharm.* **149**:93–106 (1997).
8. P. Maincent, R. Le Verge, P. Sado, P. Couvreur, and J. P. Devissaguet. Disposition kinetics and oral bioavailability of vincamin-loaded polyalkycyanoacrylate nanoparticles. *J. Pharm. Sci.* **75**:955–958 (1986).
9. D. E. Chickering III, J. S. Jacob, T. A. Desai, M. Harrison, W. P. Harris, C. N. Morrell, P. Chaturvedi, and E. Mathiowitz. Bioadhesive microspheres: III. An *in vivo* transit and bioavailability study of drug-loaded alginate and poly(fumaric-co-sebacic anhydride) microspheres. *J. Control. Release* **48**:35–46 (1997).
10. E. Mathiowitz, J. S. Jacob, Y. S. Jong, G. P. Carino, D. E. Chikering, P. Chaturvedi, C. A. Santos, K. Vijayaraghavan, S. Montgomery, M. Basset, and C. Morrell. Biologically erodable microspheres as potential oral drug delivery systems. *Nature* **386**:411–414 (1997).
11. Y. Akiyama, N. Nagahara, T. Kashihara, S. Hirai, and H. Toguchi. *In vitro* and *in vivo* evaluation of mucoadhesive microspheres prepared for the gastrointestinal tract using polyglycerol esters of fatty acids and a poly(acrylic acid) derivative. *Pharm. Res.* **12**: 397–405 (1995).
12. Y. Akiyama, N. Nagahara, E. Nara, M. Kitano, S. Iwasa, I. Yamamoto, J. Azuma, and Y. Ogawa. Evaluation of oral mucoadhesive microspheres in man on the basis of the pharmacokinetics of furosemide and riboflavin, compounds with limited gastrointestinal absorption sites. *J. Pharm. Pharmacol.* **50**:159–166 (1998).
13. M. A. Arangoa, G. Ponchel, A. M. Orecchioni, M. J. Renedo, D. Duchêne, and J. M. Irache. Bioadhesive potential of gliadin nanoparticulate systems. *Eur. J. Pharm. Sci*. **11**:333–341 (2000).
14. M. A. Arangoa. New nanoparticulate dosage forms from gliadin: development and evaluation of the bioadhesive potential. Thesis, University of Navarra, Pamplona, 1999.
15. P. Ruelle, E. Sarraf, and U. W. Kesselring. Prediction of carbazole solubility and its dependence upon the solvent nature. *Int. J. Pharm.* **104**:125–133 (1994).
16. M. A. Arangoa, M. A. Campanero, Y. Popineau, and J. M. Irache. Evaluation and characterisation of gliadin nanoparticles and isolates by reversed-phase HPLC. *J. Cereal Sci.* **31**:223–228 (2000).
17. M. A. Arangoa, M. A. Campanero, Y. Popineau, and J. M. Irache. Electrophoretic separation and characterisation of gliadin fractions from isolates and nanoparticulate drug delivery systems. *Chromatographia* **50**:243–246 (1999).
18. I. Ezpeleta, J. M. Irache, S. Stainmesse, C. Chabenat, J. Gueguen, Y. Popineau, and A. M. Orecchioni. Gliadin nanoparticles for the controlled release of all-trans-retinoic acid. *Int. J. Pharm.* **131**: 191–200 (1996).
19. B. P. Imbimbo, E. Imbimbo, S. Daniotti, D. Verotta, and G. Bassotti. A new criterion for selection of pharmacokinetic multiexponential equations. *J. Pharm. Sci.* **77**:784–789 (1988).
20. M. Rowland and T. N. Tozer. *Clinical pharmacokinetics. Concepts and applications*. Lea and Febiger, Philadelphia, 1995.
21. J. M. Lanao, M. T. Vicente, and M. L. Sayalero. Calculation of partial components of biovailability in slow release formulations using model-independent methods. *Int. J. Pharm.* **117**:113–118 (1995).
22. D. P. Callender, N. Jayaprakash, A. Bell, V. Petraitis, R. Petratienes, M. Candelario, R. Schaufele, J. M. Dunn, S. Sei, T. J. Walsh, and F. M. Balis. Pharmacokinetics of oral zidovudine entrapped in biodegradable nanospheres in rabbits. *Antimicrob. Agents Chemother.* **43**:972–974 (1999).
23. P. R. Chaturvedi. Pharmacokinetics of microparticulate systems. In S. Cohen, and H. Bernstein (eds.), *Microparticulate systems for the delivery of proteins and vaccines*, Drugs and the Pharmaceutical Sciences 77, Marcel Dekker, New York, 1996, pp. 321–347.
24. J. M. Lanao, M. T. Vicente, L. Sayalero, and A. Dominguez-Gil. A computer program (DCN) for numerical convolution and deconvolution of pharmacokinetic functions. *J. Pharmacobiodyn.* **15**:203–214 (1992).
25. S. E. Tett, D. J. Cutler, and R. O. Day. Bioavailability of hydroxychloroquine tablets assessed with deconvolution techniques. *J. Pharm. Sci.* **81**:155–159 (1992).
26. X. Wu, F. Yamashita, and M. Hashida. Deconvolution analysis for absorption and metabolism of aspirin in microcapsules. *Biol. Pharm. Bull.* **22**:1212–1216 (1999).